

## ARTICLE

# Population pharmacokinetics of letermovir following oral and intravenous administration in healthy participants and allogeneic hematopoietic cell transplantation recipients

Marita Prohn<sup>1</sup> | Anders Viberg<sup>1</sup> | Da Zhang<sup>2</sup> | Kevin Dykstra<sup>1</sup> | Casey Davis<sup>2</sup> |  
Sreeraj Macha<sup>2</sup> | Philip Sabato<sup>2</sup> | Dinesh de Alwis<sup>2</sup> | Marian Iwamoto<sup>2</sup> |  
Craig Fancourt<sup>2</sup> | Carolyn R. Cho<sup>2</sup>

<sup>1</sup>qPharmetra, Nijmegen, The Netherlands

<sup>2</sup>Merck & Co., Inc., Kenilworth, New Jersey, USA

## Correspondence

Carolyn R. Cho, Merck & Co., Inc.,  
Mailstop RY34A-500 126 E. Lincoln  
Ave., Rahway, NJ 07065, USA.  
Email: carolyn.cho@merck.com

## Present address

Anders Viberg, The Dental and  
Pharmaceutical Benefits Agency,  
Stockholm, Sweden

Da Zhang, US Food and Drug  
Administration, Silver Spring, Maryland,  
USA

Kevin Dykstra, Simulations Plus,  
Andover, Massachusetts, USA

Casey Davis, Amgen Inc., South San  
Francisco, California, USA

## Funding information

Funding for this research was provided  
by Merck Sharp & Dohme Corp.,  
a subsidiary of Merck & Co., Inc.,  
Kenilworth, NJ, USA.

## Abstract

Letermovir is indicated for prophylaxis of cytomegalovirus infection and disease in allogeneic hematopoietic stem cell transplant (HSCT) recipients. Two-stage population pharmacokinetic (PK) modeling of letermovir was conducted to support dose rationale and evaluate the impact of intrinsic/extrinsic factors. Data from healthy phase I study participants over a wide dose range were modeled to evaluate the effects of selected intrinsic factors, including pharmacogenomics; next, phase III HSCT-recipient data at steady-state following clinical doses were modeled. The model in HSCT recipients adequately described letermovir PK following both oral or i.v. administration, and was consistent with the healthy participant model at steady-state clinical doses. Intrinsic factor effects were not clinically meaningful. These staged analyses indicate that letermovir PK in HSCT recipients and healthy participants differ only with respect to bioavailability and absorption rate. The HSCT recipient model was suitable for predicting exposure for exposure–response analysis supporting final dose selection.

## INTRODUCTION

Cytomegalovirus (CMV) infection is a common herpes virus infection, which can develop into a more serious and deadly disease in immunocompromised individuals, such as hematopoietic stem cell transplant (HSCT) recipients.<sup>1</sup> Currently

available anti-CMV drugs—such as valganciclovir, ganciclovir, foscarnet, and cidofovir—are limited by their toxicity profiles and have been linked to the development of viral resistance.<sup>1–5</sup> Letermovir (MK-8228) is a novel, first-in-class inhibitor of CMV viral terminase for prophylaxis of CMV infection and disease in CMV-seropositive allogeneic HSCT

This is an open access article under the terms of the Creative Commons Attribution-NonCommercial License, which permits use, distribution and reproduction in any medium, provided the original work is properly cited and is not used for commercial purposes.

© 2021 Merck Sharp & Dohme Corp. *CPT: Pharmacometrics & Systems Pharmacology* published by Wiley Periodicals LLC on behalf of American Society for Clinical Pharmacology and Therapeutics.

recipients.<sup>6–10</sup> The letermovir recommended adult dosage is 480 mg (or 240 mg with cyclosporine [CSA]) once daily, administered orally or i.v. Given the urgent unmet medical need for new anti-CMV treatments, approval of letermovir was based on the results of a single phase III randomized, double-blind, placebo-controlled trial (NCT02137772).<sup>9,11</sup> Overall, letermovir has been shown to be generally well-tolerated, with a safety profile generally similar to that of placebo.<sup>8,11–14</sup>

Phase I studies in healthy participants showed that letermovir pharmacokinetics (PKs) are nonlinear and time-dependent, characterized by greater than dose-proportional increases in exposure, limited accumulation upon multiple dosing, and large variability in absorption profiles upon oral administration.<sup>9,15</sup> Letermovir clearance occurs primarily via biliary excretion as unchanged parent. Consistent with this, letermovir is a substrate for the hepatic drug transporter organic-anion-transporting polypeptide family 1 member B1 (*OATP1B1*), and has also been shown to be metabolized via UDP glucuronosyltransferase family 1 member A1 (*UGT1A1*)-mediated glucuronidation.<sup>9</sup> Letermovir exposure is increased by co-administration with CSA, likely due to CSA inhibition of liver uptake transporters *OATP1B1/3*, resulting in the recommended letermovir dose being reduced to 240 mg once daily in cases of CSA co-administration.<sup>16</sup>

To characterize letermovir PK and influential factors, we conducted population pharmacokinetic (popPK) modeling, developed in two stages: (1) a healthy participant model of letermovir exposure covering a broad range of doses and different dosing regimens, using pooled intensive PK data from healthy participants in 12 phase I studies; and (2) a separate HSCT recipient popPK model to describe the steady-state PK of letermovir at clinical doses in HSCT recipients, using data from the phase III trial, pooled with steady-state PK data with the same dosing from a phase IIb trial (240 mg with CSA) and phase I trials (480 mg without CSA).

The healthy participant model was primarily used to characterize PK in healthy participants over a wide range of dose levels following both i.v. and oral administration, search for influential intrinsic and extrinsic factors, and guide the design of the HSCT recipient model. The HSCT recipient model was primarily used to characterize PK in HSCT recipients, determine post hoc steady-state PK parameter values, provide exposure estimates for subsequent exposure–response analysis, and, ultimately, support the rationale for clinical dose selection.

Here, we describe the development and findings of both models.

## METHODS

### Data sources

For the healthy participant (phase I) model, PK data from healthy participants were sourced from 12 phase I studies

### Study Highlights

#### WHAT IS THE CURRENT KNOWLEDGE ON THE TOPIC?

Letermovir is a first-in-class cytomegalovirus (CMV) viral terminase inhibitor indicated for the prophylaxis of CMV infection and disease following allogeneic hematopoietic stem cell transplant (HSCT).

#### WHAT QUESTION DID THIS STUDY ADDRESS?

The aim of this analysis was to characterize the population pharmacokinetics (popPKs) of letermovir in healthy phase I trial participants and in HSCT recipients, in order to support dose rationale and assess the potential impact of intrinsic and extrinsic covariates.

#### WHAT DOES THIS STUDY ADD TO OUR KNOWLEDGE?

Letermovir PK was similar between healthy participants and HSCT recipients, except for disease-related differences in bioavailability and absorption. Using the popPK models, it was possible to predict confidently the PK and variability of the approved dosing regimen in HSCT recipients.

#### HOW MIGHT THIS CHANGE DRUG DISCOVERY, DEVELOPMENT, AND/OR THERAPEUTICS?

When given either orally or i.v., with or without cyclosporine A at the recommended clinical dose to HSCT recipients, the PK of letermovir is sufficiently described using a linear two-compartment model with delayed absorption. No covariates were found to have clinically relevant effects on letermovir PK in healthy participants.

( $n = 280$ ; Table 1). For the HSCT recipient (phase III) model, steady-state PK data from HSCT recipients were sourced from one phase III trial ( $n = 350$ ), one phase IIb trial ( $n = 13$ ), and three phase I trials ( $n = 36$ ; Table 1).

### PopPK model development

Nonlinear mixed effects modeling (NONMEM version 7.3; ICON, plc, Dublin, Ireland) was used to develop both popPK models. This approach estimates the typical (mean) value of parameters as well as their between-subject variances. During model development, a difference in objective function value (OFV),  $\Delta$ OFV of 3.84 was used between 2 nested models differing in one parameter (corresponding to a nominal  $p$  value  $< 0.05$ ). A model was considered stable if two or

**TABLE 1** Comparison of healthy participant (phase I) and HSCT recipient (phase III) model datasets

Property	Category	Model	
		Phase I	Phase III
Studies	Phase I	12	3
	Phase IIb	0	1
	Phase III	0	1
Subjects by disease state, <i>n</i> (%)	Healthy	280 (100)	36 (9)
	HSCT	0	363 (91)
Gender, <i>n</i> (%)	Female	254 (91)	190 (48)
	Male	26 (9)	209 (52)
Age, years; median (range)		30 (18–59)	51 (18–75)
Weight, kg; median (range)		66 (45–99)	75 (35–142)
Dose range, mg		30–960	240–480
CsA co-administration		No	Yes
PK samples by disease state, <i>n</i> (%)	Healthy	9020 (100)	444 (15)
	HSCT	0	2444 (85)
PK samples by administration route, <i>n</i> (%)	i.v.	2629 (29)	322 (11)
	Oral	6391 (71)	2566 (89)
PK samples by dosing, <i>n</i> (%)	Single-dose	4680 (52)	0
	Multiple-dose	4340 (48)	2888 (100)
PK density by subjects, %	Intensive	100	31
	Sparse	0	69

Abbreviations: CsA, cyclosporine A; HSCT, hematopoietic stem cell transplant; PK, pharmacokinetic.

more different sets of initial estimates resulted in similar parameter estimates and OFV. The final model was determined on the basis of maximized likelihood (lowest stable OFV, physiological plausibility of parameter values, successful numerical convergence, good parameter precision, and an acceptable visual predictive check [VPC]).<sup>17</sup>

### Covariate analysis

Identification of covariate effects on PK parameters was done using a stepwise selection procedure using the SCM function in Perl-speaks-NONMEM (PsN) version 4.2.0.<sup>18</sup> This procedure involves stepwise testing of linear and nonlinear relationships in a forward inclusion and backward exclusion procedure. A  $\Delta$ OFV of 6.63 (nominal *p* value < 0.01) was used for an effect to be included in the model during forward inclusion and  $\Delta$ OFV of 10.83 (nominal *p* value < 0.001) for retention of an effect during backward elimination. To minimize the risk of false positives, only clinically plausible covariate relationships were evaluated.

At each stage, model development proceeded until no further improvement in fit was seen. The final model parameters and covariate selection were determined using the full dataset with the final structural model.

### Healthy participant (phase I) popPK model development

First, separate models describing oral and i.v. single-dose PK data in healthy participants were developed, and then expanded to include multiple-dose PK data. Finally, the oral and i.v. models were merged into a structural model describing the full dataset. Efforts were made to describe the supra-proportional dose nonlinearity previously observed, as well as the difference in absorption profiles observed following multiple doses of letermovir. Nonlinear relationships were investigated on elimination and on distribution parameters. Different absorption models, including the Erlang model<sup>19</sup> and the transit compartment absorption model (TCAM),<sup>20</sup> were tested.

### HSCT recipient (phase III) popPK model development

The model was developed in a stepwise fashion; first, with steady-state phase I PK data from healthy participants, thereafter, including phase II and III PK data from HSCT recipients with multiple samples from at least one dosing interval, and last, including all available HSCT-recipient (phase III) PK data.

Additional methodology is provided in the accompanying Supplementary Information, including full details

on phase I and III model development, model diagnostics and qualification, covariates, and letermovir exposure estimation.

## RESULTS

### Healthy participant (phase I model) popPK

#### Modeling population

The full dataset used for model development included 9020 PK observations obtained in 280 healthy participants. The analysis excluded 174 PK observations below the lower limit of quantification (LLOQ; 1.9% of samples). The demographics of the analysis set are summarized in Table 1. Most of the phase I studies recruited only female participants due to preclinical testicular toxicity in rats; therefore, greater than 90% of subjects in the pooled healthy-participant dataset were female.

#### Model development

Overall, letermovir PK was best described by a four-compartment model with concentration-dependent nonlinear clearance (CL) and intercompartment clearance to the first peripheral compartment ( $Q_1$ ) and auto-induction of CL. Several models, such as the Erlang model<sup>19</sup> and the TCAM,<sup>20</sup> were considered to describe letermovir absorption after oral administration, of which the TCAM best described the data. Interindividual variability (IIV) was included on key parameters (maximal clearance rate [ $CL_{max}$ ], central volume of distribution [ $V_1$ ], first peripheral volume of distribution [ $V_2$ ], maximal intercompartment clearance to the first peripheral compartment [ $Q_{1max}$ ], bioavailability [ $F_1$ ], and mean transit time [MTT]). Exploration of both oral and i.v. data showed a greater than proportional increase in exposure with dose. Additionally, it was noted in exploratory plots that trough concentrations following multiple oral doses increased at first, as expected with slow elimination relative to the dosing interval, and then decreased over time. This observation was incorporated in the model with an induction effect on CL.

Residual variability was described using a proportional residual error model. The model included an effect of Asian descent on volume of distribution ( $V_d = V_1 + V_2 + V_3 + V_4$ ), and a body weight effect on  $V_d$  and  $CL_{max}$ . The final model is represented graphically in Figure 1a and parameter estimates are shown in Table 2.  $F_1$  of letermovir after oral administration was estimated to be 93.8%, with MTT in the TCAM model for a 240 mg oral dose estimated to be 1.4 h, with a first-order absorption rate of 0.66/h.

### Model qualification

The model demonstrated appropriate agreement between predicted and observed values (Figure S1a). The conditional weighted residuals (CWRES) were randomly scattered around the predicted range and over time, as expected (Figure S1b). The normal quantile-quantile plot and a density plot of the CWRES indicated that the residuals were normally distributed, with a mean and variance of approximately 0 and 1, respectively. There was no significant difference in individual deviation (ETA) values between the different genetic polymorphisms, or for age or gender (data not shown).

A prediction-corrected VPC stratified by administration route and regimen (single-dose or multiple-dose) showed that the model adequately described the data obtained from healthy participants (Figure S2). Model fit was good over the dose range of 60–720 mg; at the low (30 mg) and high (960 mg) end of the dose range analyzed, the model did not adequately describe the full concentrations versus time profiles (data not shown); however, goodness of fit (GOF) plots did not demonstrate structural bias in the model.

### Impact of covariates

Statistically significant effects of body weight on both  $CL_{max}$  and  $V_d$ , and Asian descent on  $V_d$  (27.6% lower  $V_d$  in Asian participants), were identified (Figure S3). It was predicted that Asian participants would have a 33.2% higher exposure than White participants after treatment with multiple oral doses of 480 mg letermovir (area under the concentration-time curve [AUC] of  $1.08 \times 10^5$  ng·h/ml and  $8.11 \times 10^4$  ng·h/ml, respectively). When assuming an identical average body weight of 67.1 kg in both populations, letermovir exposure was predicted to be 10.1% higher in Asian participants compared with White participants. These increases in exposure were determined not to be clinically relevant. Although most of the healthy participants were female, gender was not found to have a significant covariate effect on PK, and individual parameter estimates stratified by gender were not significantly different. In total, 224 participants had available single nucleotide polymorphism data for *OATP1B1* (rs4149056 and rs2306283) and *UGT1A1* (rs4148323). These functional variants had no statistically significant effect on letermovir exposure and they were not included in the final model.

### Exposure predictions

After oral administration, letermovir-predicted exposure (AUC) increased nonlinearly with dose, both after

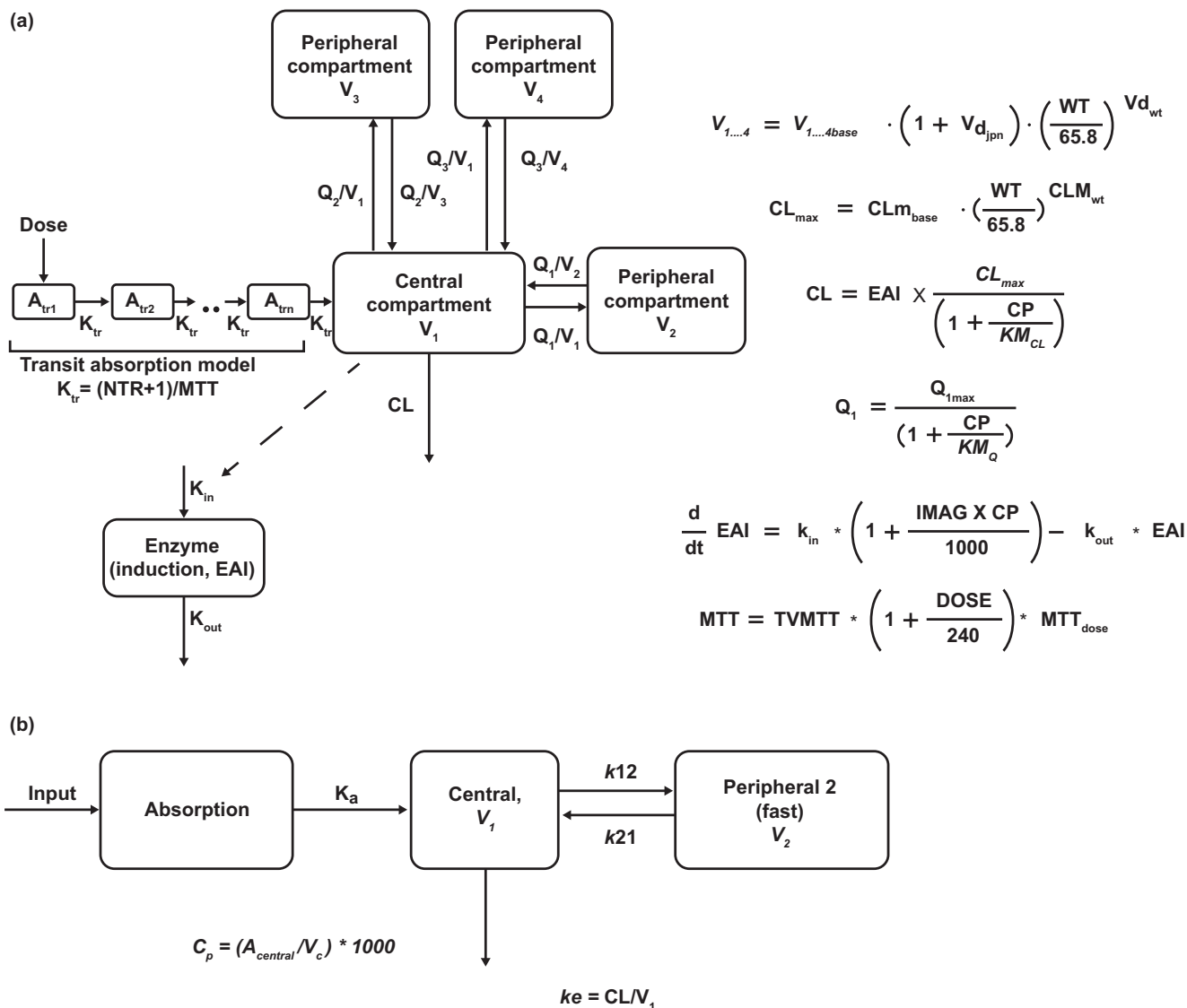


**FIGURE 1** Graphical representation of the (a) healthy participant (phase I model), and (b) HSCT recipient (phase III model) popPK models.  $A_{tr}$ , drug amount in a transit compartment; CL, clearance;  $CL_{max}$ , maximal clearance rate;  $CL_{m_{base}}$ ,  $CL_{max}$  for a typical 65.8 kg subject;  $CLM_{wt}$ , exponent describing the weight effect on  $CL_{max}$ ;  $C_p$ , letermovir plasma concentration; EAI, induction compartment amount; HSCT, hematopoietic stem cell transplant; IMAG, scalar of the induction effect;  $k_{in}$ , production rate induction compartment;  $KM_{CL}$ , Michaelis-Menten constant for clearance;  $KM_Q$ , Michaelis-Menten constant for intercompartmental clearance;  $k_{out}$ , elimination rate induction compartment;  $K_{tr}$ , transit rate constant; MTT, mean transit time;  $MTT_{dose}$ , dose effect on MTT; NTR, number of transit compartments; popPK, population pharmacokinetics;  $Q_1$ , intercompartment clearance to the first peripheral compartment;  $Q_{1max}$ , maximal intercompartment clearance to the first peripheral compartment;  $Q_2$ , intercompartment clearance to the second peripheral compartment;  $Q_3$ , intercompartment clearance to the third peripheral compartment; TVMTT, MTT for a typical dose of 240 mg;  $V_1$ , central volume of distribution;  $V_2$ , first peripheral volume of distribution;  $V_3$ , second peripheral volume of distribution;  $V_4$ , third peripheral volume of distribution;  $V_{1-4base}$ ,  $V_{1-4}$  for a typical 65.8 kg subject;  $V_d$ , volume of distribution (sum of  $V_1$ ,  $V_2$ ,  $V_3$ , and  $V_4$ );  $V_{d_{base}}$ ,  $V_d$  for a typical 65.8 kg subject;  $V_{d_jpn}$ , Asian effect on  $V_{d_{base}}$ ;  $V_{d_{wt}}$ , weight effect on  $V_d$ ; WT, wild type

single-dose and multiple-dose administration (Figure 2). The maximum letermovir concentration ( $C_{max}$ ) increased almost proportionally with dose between 30 and 960 mg after single-dose and multiple-dose oral administration (Figure 2a). After both single-dose and multiple-dose i.v. administration, letermovir AUC and  $C_{max}$  increased nonlinearly with dose (Figure 2b).

### HSCT recipient (phase III model) popPK

#### Modeling population

The full dataset used for phase III model development included 2888 sample concentration observations from 399 HSCT recipients; most samples were obtained from the

**TABLE 2** Parameter estimates of the healthy participant (phase I) popPK model

Parameter	Alias	Estimate	Relative SE (%)	Bootstrap estimate	Bootstrap 95% CI
Clearance $V_{max}$ , L/h	$CL_{max}$	12.3	2.60	12.2	11.3–13.3
Weight effect on clearance $V_{max}$	$CL_{max-wt}$	0.566	26.4	0.560	0.376–0.741
Central volume of distribution, L	$V_1$	7.46	6.30	7.45	6.94–7.89
Weight effect on $V_d$	$V_{d-wt}$	0.667	10.9	0.656	0.452–0.854
Asian effect on $V_d$	$V_{d-jpn}$	−0.281	8.80	−0.280	−0.334 to −0.227
Number of transit compartments	NTR	3.58	1.70	3.60	3.12–4.09
Mean transit time, h	MTT	1.04	4.20	1.04	0.949–1.14
Dose effect on MTT	$MTT_{dose}$	0.344	11.5	0.340	0.258–0.433
Intercompartment clearance $V_{max}$ , L/h	$Q_{1max}$	4.39	4.90	4.41	3.93–4.95
Peripheral volume, L	$V_2$	61.6	4.80	61.5	55.3–68.2
Intercompartment clearance, L/h	$Q_2$	31.3	12.3	31.4	27.2–36.6
Peripheral volume, L	$V_3$	12.1	4.20	12.2	11.4–12.9
Michaelis-Menten constant, ng/ml	$KM_{CL}$	$2.68 \times 10^3$	4.50	$2.72 \times 10^3$	$2.20 \times 10^3$ – $3.41 \times 10^3$
Michaelis-Menten constant, ng/ml	$KM_{Q1}$	$5.63 \times 10^3$	10.3	$5.35 \times 10^3$	$3.81 \times 10^3$ – $7.32 \times 10^3$
Turnover rate induction, /h	$K_{out}$	0.00783	NA	0.00775	0.00580–0.00966
Slope of induction effect	IMAG	0.0829	NC	0.0837	0.0672–0.102
Bioavailability	$F_1$	0.938	2.10	0.938	0.906–0.974
Intercompartment clearance, L/h	$Q_3$	4.91	4.90	4.91	4.49–5.39
Peripheral volume, L	$V_4$	19.0	4.00	19.2	17.4–21.2
IIV, clearance $V_{max}$	$IIV-CL_{max}$	0.0647	9.90	0.0641	0.0533–0.0766
IIV, central volume	$IIV-V_1$	0.0642	30.7	0.0613	0.0387–0.0977
IIV, mean transit time	$IIV-MTT$	0.0841	14.2	0.0836	0.0700–0.0976
IIV, intercompartmental clearance	$IIV-Q_{1max}$	0.155	16.0	0.159	0.126–0.203
IIV, peripheral volume	$IIV-V_2$	0.224	11.4	0.224	0.184–0.273
IIV, bioavailability	$IIV-F_1$	0.0323	13.3	0.0323	0.0232–0.0425
Proportional residual variability, %	Prop error	0.283	0.300	0.282	0.271–0.294

Note: Relative standard error was not calculated for log-transformed parameters.

Abbreviations: CI, confidence interval;  $CL_{max}$ , maximal clearance rate;  $F_1$ , bioavailability; IIV, interindividual variability; IMAG, scalar of the induction effect;  $KM_{CL}$ , Michaelis-Menten constant for clearance;  $KM_{Q1}$ , Michaelis-Menten constant for intercompartmental clearance;  $K_{out}$ , elimination rate induction compartment; MTT, mean transit time;  $MTT_{dose}$ , dose effect on MTT; NA, not applicable; NC, not calculated; NTR, number of transit compartments; popPK, population pharmacokinetics;  $Q_{1max}$ , maximal intercompartment clearance to the first peripheral compartment;  $Q_2$ , intercompartment clearance to the second peripheral compartment;  $Q_3$ , intercompartment clearance to the third peripheral compartment;  $V_1$ , central volume of distribution;  $V_2$ , first peripheral volume of distribution;  $V_3$ , second peripheral volume of distribution;  $V_4$ , third peripheral volume of distribution;  $V_d$ , volume of distribution (sum of  $V_1$ ,  $V_2$ ,  $V_3$ , and  $V_4$ );  $V_{max}$ , maximum elimination rate; WT, wild type.

phase III dataset (2315/2888, 80.2%). Demographics of the full dataset are summarized in Table 1. In total, 53 PK observations below the LLOQ were excluded (1.8% of samples).

## Model development

Steady-state PK data from healthy participants from phase I studies were used to develop the base structural model ( $n = 36$ , 444 observations). Oral and i.v. data were fitted simultaneously. A sufficient model fit was obtained using a two-compartment model with first-order absorption and linear elimination. Next, data from HSCT recipients from the phase IIb study ( $n = 13$ , 129 observations) and the rich

sampling subset from the phase III study ( $n = 74$ , 369 observations) were added. The model based on the steady-state data obtained in healthy participants did not adequately describe the HSCT-recipient (phases II and III) data, and further model refinement was required to adequately describe letermovir PK in HSCT recipients. Estimating a separate CL when co-administering letermovir with CSA improved model fit ( $\Delta OFV -88.1$ ). Separate bioavailability for healthy participants and for CSA treatment also improved model fit ( $\Delta OFV -18.4$  and  $-10.5$ , respectively). Models in which the bioavailability for healthy participants was estimated were numerically unstable and resulted in bioavailability estimates close to 100%. For comparison, bioavailability in healthy participants from the phase I model

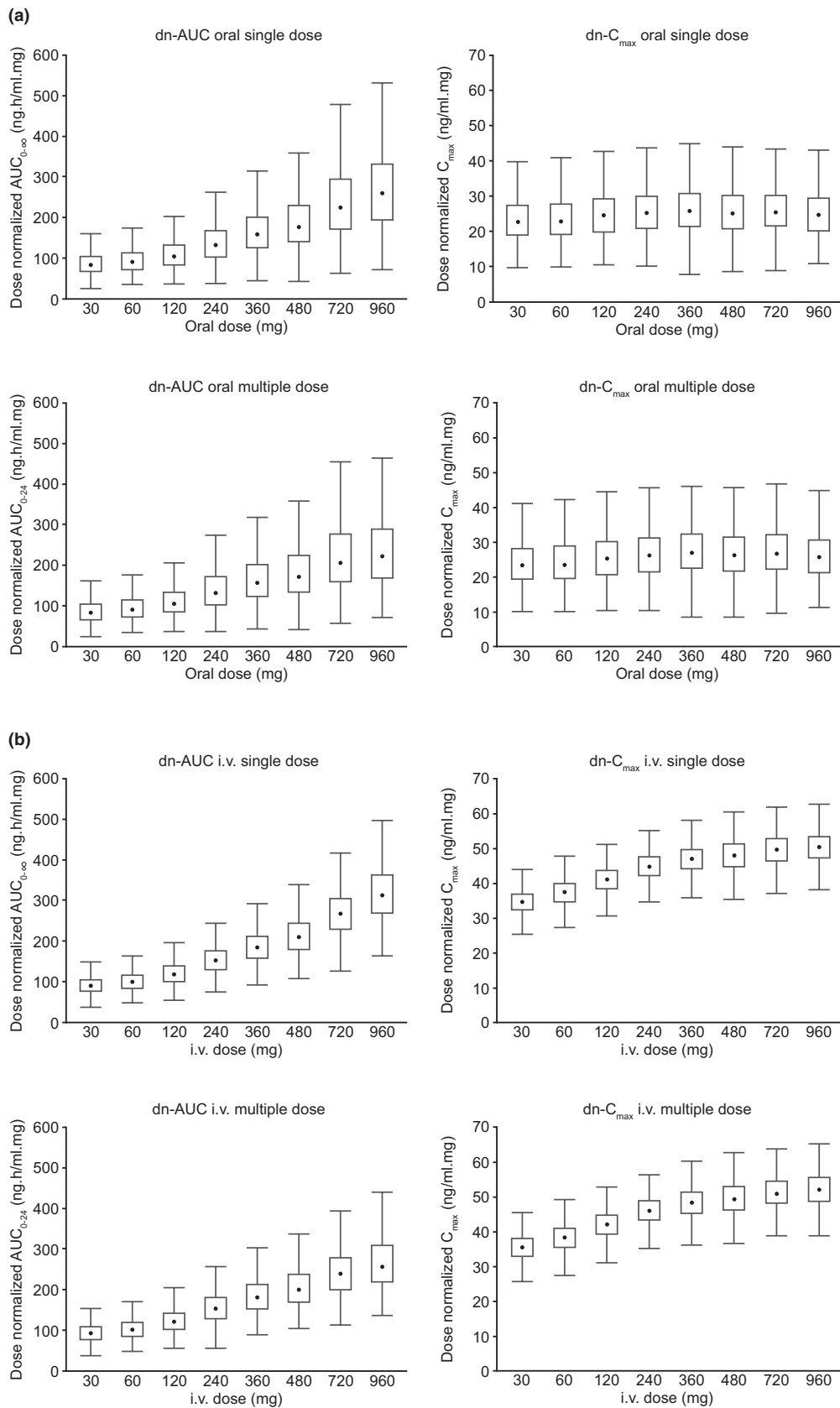


**FIGURE 2** Simulated letemovir exposure using the healthy participant (phase I) popPK model after single-dose or multiple-dose: (a) oral administration; (b) i.v. administration. Box and whisker plot: the dot is the sample median, the boxes define the interquartile range, whiskers extend to 1.5 times the interquartile range. AUC, area under the concentration-time curve;  $C_{max}$ , maximum concentration (multiple-dose  $C_{max}$  at steady-state); dn, dose normalized; popPK, population pharmacokinetics

Parameter	Estimate	CV%	95% CI	95% bootstrap CI
CL non-CSA treatment, L/h	4.84	—	(4.3–5.45)	4.29–5.35
CL CSA treatment, L/h	3.38	—	(2.8–4.09)	2.7–3.98
Central volume, L	19.7	—	(17.6–22.1)	17.8–22.4
Peripheral volume, L	25.8	—	(19.1–34.9)	19.3–37
Intercompartment CL, L/h	1.54	—	(1.17–2.04)	1.17–2.02
Bioavailability without CSA	0.346	—	(0.278–0.42)	0.277–0.446
Bioavailability HP	1.00	—	—	1–1
Bioavailability with CSA	0.849	—	(0.561–0.961)	0.644–1
Absorption rate, 1/h	0.150	—	(0.104–0.215)	0.105–0.256
Absorption rate HP, 1/h	1.26	—	(0.933–1.71)	0.967–1.91
Absorption lag, h	0.674	—	(0.59–0.769)	0.569–0.776
Proportional residual variability	0.517	12.2	(0.394–0.641)	0.379–0.609
Additive residual variability, ng/ml	383.0	22.2	(216–550)	206–615
Proportional residual variability phase I	0.244	6.4	(0.213–0.274)	0.214–0.276
Proportional residual variability sparse data	0.612	6.6	(0.532–0.691)	0.525–0.697
Additive residual variability sparse data, ng/ml	267.0	9.6	(217–318)	207–319
Asian effect peripheral volume	0.609	—	(0.53–0.7)	0.525–0.712
IIV, CL	0.0605	17	(0.0403–0.0807)	0.0372–0.0819
IIV, bioavailability	0.137	24.5	(0.0714–0.203)	0.0674–0.21
IIV, peripheral volume	0.229	36.7	(0.0643–0.393)	0.0906–0.591
IIV, absorption rate	0.719	41.4	(0.136–1.3)	0.363–1.67
IOV, bioavailability	0.197	15.9	(0.136–0.259)	0.129–0.266

Note: CV% for parameters that are log or logit transformed during estimation are not reported.

Abbreviations: CI, confidence interval; CL, clearance; CSA, cyclosporine A; CV, coefficient of variation; HP, healthy participant; HSCT, hematopoietic stem cell transplant; IIV, interindividual variability; IOV, inter-occasion variability; popPK, population pharmacokinetic.

was estimated at 93.8% (95% confidence interval, 90.6%–97.4%). Therefore, to stabilize the model, bioavailability was fixed to 100%.

The remaining sparse HSCT-recipient (phase III) data ( $n = 275$ , 1530 observations) were added to the dataset, and separate residual error parameters were included for healthy participants and HSCT recipients. Estimation of a separate absorption rate ( $K_a$ ) for healthy participants resulted in a 63-unit reduction in OFV. Interoccasion variability (IOV) was included on bioavailability to account for the 100-fold difference in minimum concentration ( $C_{trough}$ ). IIV were tested on all parameters and found to be significant on CL, bioavailability,  $V_2$ , and  $K_a$ . Adding IIV on  $V_1$  did not result in a better model fit.

The stepwise covariate search identified a lower  $V_2$  for Asian subjects. Adding the effect of body weight on CL without the Asian effect on  $V_2$  or replacing the Asian

**TABLE 3** Parameter estimates of the HSCT recipient (phase III) popPK model

covariate on  $V_2$  with body weight did not improve the model.

The final model described the PK of letermovir using a two-compartment distribution with linear elimination and first-order absorption with a lag (Figure 1b). Parameter estimates are listed in Table 3. Healthy participants had very high bioavailability and an almost 10-fold faster absorption rate than HSCT recipients. Based on the final model, letermovir bioavailability in HSCT recipients was approximately 35% when administered alone, and increased to approximately 85% following co-administration with CSA. Corresponding values for CL were 4.8 and 3.4 L/h, respectively. VPCs indicated that, overall, the model predicted the observed data well (Figure S4a), although  $C_{max}$  during i.v. administration was not fully captured for the healthy-participant data. Plots of CWRES versus population predictions by route and cotreatment of CSA are shown in Figure S4b.

## Model robustness and sensitivity

Because of the high variability in PK in HSCT recipients, additional robustness and sensitivity analyses were conducted to understand the robustness of exposure estimates from the model.

Comparing PK parameter values calculated by noncompartmental analysis (NCA) versus exposure metrics calculated from the popPK model, there was good agreement between predicted AUC from 0 to 24 h postdose at steady state ( $AUC_{ss}$ ) but not  $C_{max}$ . In particular, virtually all of the phase III model-predicted  $C_{max}$  values for orally administered letermovir fell below the observed values (Figure S5).

In order to assess whether exposure predictions differ between participants with rich PK sampling and those with sparse sampling, the weighted individual average  $AUC_{ss}$  predictions for phase III participants were compared by sampling regimen (Figure S6a). The distribution of  $AUC_{ss}$  values appeared to be similar between participants with rich versus sparse sampling, although the variability in the sparsely sampled participants was higher than in participants who provided frequent samples after 1 week of treatment.

Many HSCT recipients in the phase III trial provided only trough PK samples, and the data from these observations showed substantial variability. To determine whether the model appropriately accounted for intersubject variability, the within-participant average  $C_{trough}$  variability from the oral HSCT-recipient data was compared with the expected variability from the model. A comparison of the observed within-subject geometric means with the simulated values accounting only for IIV is shown in Figure S6b. The agreement in the distributions of the observed within-subject geometric mean trough values with the simulated distribution was very good, supporting appropriate apportionment of IIV, IOV, and residual variability in the model.

Accounting for variability, comparisons with NCA, and the effects of rich versus sparse sampling, model-based population predictions of  $AUC_{ss}$  and  $C_{trough}$ , and individual AUC predictions were well supported. Therefore, the model was deemed fit for the purpose of evaluating predicted letermovir exposure resulting from different regimens and in different populations. Further, individual post hoc estimates of  $AUC_{ss}$  were accepted to be used in subsequent exposure–response analyses for safety and efficacy end points.

## Exposure predictions

Simulations showed that the median  $AUC_{ss}$  was predicted to be 34,400 ng·h/ml (90% prediction interval [PI] 16,900–73,700) for 480 mg/day oral letermovir, and 60,800 ng·h/ml (90% PI 28,700–122,000) for 240 mg/day oral letermovir co-administered with CSA. Following i.v. administration, the predicted median  $AUC_{ss}$  was 100,000 ng·h/ml (90% PI 65,300–148,000) for 480 mg/day letermovir, and 70,300 ng·h/ml

(90% PI 46,200–106,000) for 240 mg/day letermovir with CSA co-administration (consistent with a 50% reduction in dose and approximately 30% lower CL with CSA). Histograms of individual and simulated exposures are shown in Figure 3a, and box-whisker plots of exposure with different letermovir regimens are shown in Figure 3b. Simulated temporal letermovir PK profiles for non-Asian (White, Black, Hispanic, and other) and Asian (Japanese and Asian participants from other countries) participants following different dosing regimens are shown in Figure S7.

## DISCUSSION

This two-staged popPK analysis supported the evaluation of intrinsic and extrinsic factors for letermovir dose recommendation. Phase III popPK model estimates of AUC adequately described the observed data, and predicted letermovir exposure resulting from different regimens and populations, including the observed phase I AUC determined by NCA following administration of clinical doses in healthy participants.

The final phase III popPK model described steady-state trough PK using a two-compartment model with linear elimination and linear absorption with a lag time. The model adequately described letermovir steady-state AUC PK in HSCT recipients who receive the drug orally or i.v., alone or concomitantly with CSA. Based on the estimated absorption delay and rates, letermovir appears to be primarily absorbed in the small intestine, but not the stomach, with slower absorption in HSCT recipients compared with healthy participants. The lower bioavailability and lower exposures of letermovir following oral administration in HSCT recipients appear to be consistent with trends observed with other drugs frequently given to this patient population (e.g., CSA, mycophenolic acid, and posaconazole).<sup>21–23</sup> Letermovir-treated participants receiving concomitant CSA had higher oral bioavailability and lower CL than participants not treated with CSA. It is possible that the mechanism causing a reduction in CL also reduces first-pass metabolism in CSA-treated participants, resulting in an increase in apparent bioavailability. The effect of CSA on i.v. letermovir appeared to be less pronounced than that observed on oral letermovir, resulting in lower exposures with 240 mg i.v. letermovir and CSA compared with 480 mg i.v. letermovir alone.

The phase I popPK model for letermovir described phases I–III trial data covering a wide range of concentrations (1 ng/ml to > 10,000 ng/ml). The data exhibited considerable variability, both between and within subjects, with repeated trough concentrations covering a greater than 10-fold range in some subjects. The appropriateness of the four-compartment model structure was supported by a significant  $\Delta OFV$  and by observed PK over the dose range investigated. At the lowest (30 mg) and highest

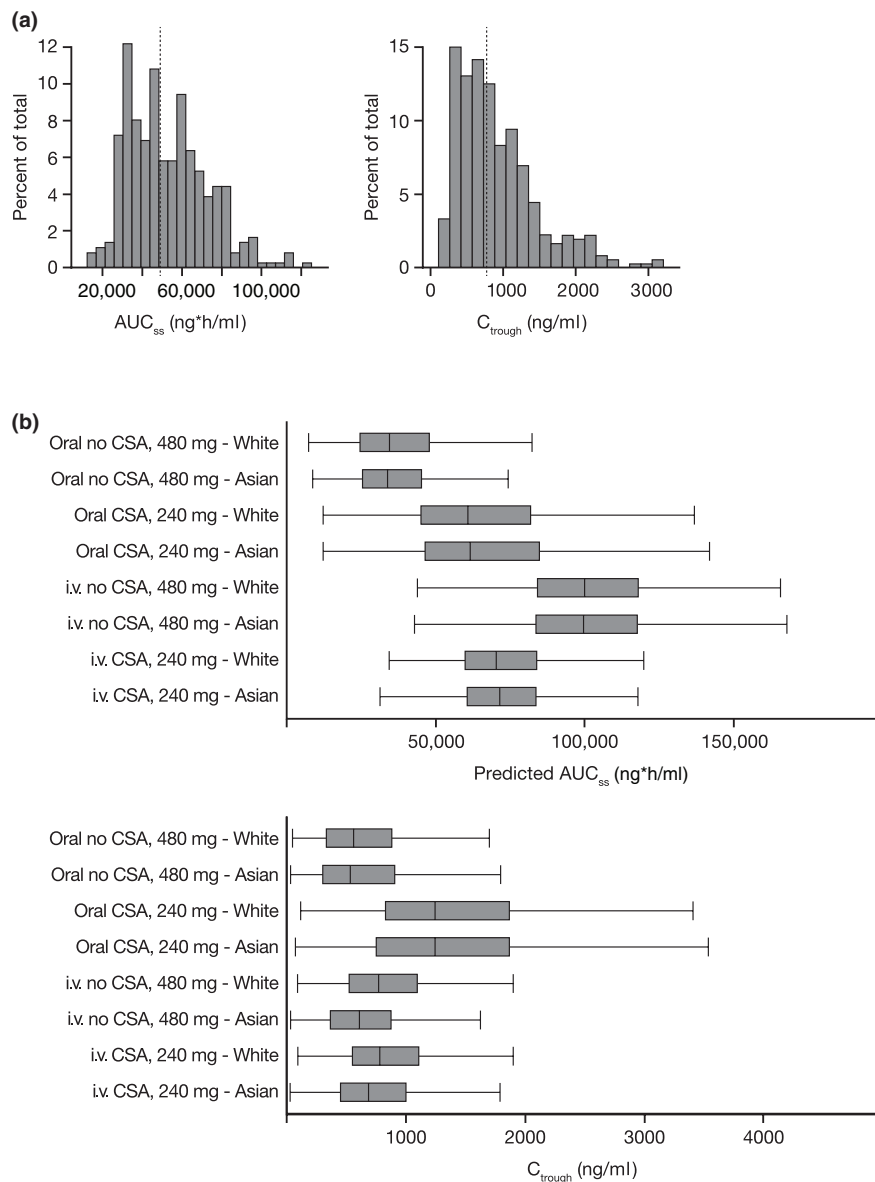


**FIGURE 3** HSCT recipient (phase III) popPK model predictions of letermovir exposure in HSCT recipients: (a) histograms of individual predicted letermovir  $AUC_{ss}$  and  $C_{trough}$ ; (b) box-whisker plots of simulated  $AUC_{ss}$  and  $C_{trough}$  following different letermovir dosing regimens.  $AUC_{ss}$ , area under the concentration-time curve from 0 to 24 h postdose at steady-state; CSA, cyclosporine A;  $C_{trough}$ , minimum concentration; HSCT, hematopoietic stem cell transplant; popPK, population pharmacokinetics

(720 mg twice daily) doses, the model did not describe the full concentration versus time profiles well; however, GOF plots did not demonstrate structural bias in the model. Within the proposed therapeutic range for letermovir of 480 mg daily by i.v. or oral administration, the model described the observed PK well. Letermovir exposures achieved in healthy participants were consistent with those observed with the 480 mg i.v. dose in HSCT recipients.

Differences between the phase I and phase III popPK models should not be interpreted as indicative of a difference in disposition between healthy participants and HSCT recipients. Rather, the differences in the models reflect different purposes, sampling schedules, and dose ranges of letermovir. Nonlinearity in letermovir PK is largely absent over the range of exposures encountered with the clinical dose. The mechanism of letermovir dose nonlinearity is not fully understood at this time but is hypothesized to be related to saturation of one

or more transporters. Physiologically-based PK modeling indicated that saturation of *OATP1B*-mediated hepatic uptake, rather than saturation of typical elimination processes, best described the mechanism of letermovir nonlinear PK.<sup>24</sup>

A comparison of the phase I and phase III popPK models has been performed previously<sup>25</sup> to understand and compare the appropriateness of the models to explain the observed clinical data and support the clinical dose recommendation. The study compared the model structures, parameters, and predictive performance in the overlapping domain of healthy participants following administration of the clinical dose of letermovir at steady-state. Results demonstrate that the phase III model may be considered a simplification of the phase I model assuming that at the clinical dose, letermovir PK is in a linear range such that clearance from the central compartment is saturating (constant) and nonlinear distribution between the central and peripheral compartments can be approximated by

a first-order constant. The comparison confirms that healthy participants and HSCT recipients have similar postabsorption PK properties and that PK in the two populations differs with respect to bioavailability and absorption rate.

Covariate analysis of the phase III model indicated that individuals of Asian origin had lower  $V_2$  compared with White participants. Consistent with this finding, Asian participants had a 28.1% lower  $V_d$  compared with White participants based on the healthy participant (phase I) model. Both  $CL_{max}$  and  $V_d$  were also impacted by body weight, whereas gender was found to have no significant impact on letermovir PK in healthy participants. Because of differences between median body weight of Asian (56.6 kg) versus White (67.1 kg) participants, additional simulations were performed to predict a combinatorial effect of 33.2% higher exposure in Asian participants compared with White participants. Nonetheless, although point estimates of median letermovir exposure differed between White and Asian participants, there was a high degree of overlap in the prediction intervals, consistent with observations in the phase III popPK analysis for Asian/White participants; thus, the differences in exposure were determined not to be clinically relevant. Of note, the phase I popPK model also evaluated Japanese ethnicity ( $n = 30$ ) as a covariate, but this was later replaced by Asian ethnicity ( $n = 33$ ), which slightly improved the model.

In addition to the standard GOF and simulation-based model qualification steps, additional analysis of phase III popPK model robustness was conducted by checking the agreement of model exposure predictions with several independently derived exposure metrics. NCA of the data from healthy participants in phase I studies, along with data obtained from the subset of HSCT recipients in whom frequent observations were obtained following a single dose, was compared with the model-predicted exposure. This analysis suggested good agreement of the predicted  $AUC_{ss}$  from the individual CL estimates from the model, with the  $AUC_{ss}$  calculated via NCA. Conversely,  $C_{max}$  was not well predicted by the model. It is noteworthy that the model included between-subject variability in CL and  $V_2$  but not in  $V_1$ . Because  $V_1$  is the main determinant of  $C_{max}$  following i.v. administration, it is not surprising that variability in  $C_{max}$  was not well captured by the model. Furthermore, the current two-compartment model did not offer a sufficiently comprehensive description of data derived from i.v.-treated participants to characterize  $C_{max}$  after i.v. administration. A three-compartment model may be required to prevent underprediction of  $C_{max}$ ; however, estimation of CL and prediction of  $AUC_{ss}$  were the main modeling objectives and were achieved adequately with the two-compartment model, without overparameterization.

A second robustness analysis of the phase III popPK model compared the distribution of  $AUC_{ss}$  in participants contributing rich data with participants contributing only trough measurements. This analysis suggested similar distributional

characteristics between the two study populations, supporting the use of  $AUC_{ss}$  as a predictive exposure metric. A final examination compared the intersubject distribution in average  $C_{trough}$  obtained from repeated observations within individual participants (given oral treatment) to a distribution derived from the PK model, including only the effects of IIV. This analysis showed that  $C_{trough}$  measurements were well-predicted by the model and, further, suggested that the random effects model properly accounts for variability between and within individual participants.

Taken together, these assessments showed that the phase III PopPK model describes the data adequately, and is well-suited for the purpose of predicting  $AUC_{ss}$  and  $C_{trough}$  for exposure–response analysis and to support identification of appropriate letermovir doses for prophylactic treatment of HSCT recipients. Dose justification was adequately supported with these parameters, and not negatively impacted by the lack of  $C_{max}$  predictions. Because participants in the phase III trial switched between i.v. and oral administration, as well as from dosing letermovir alone or in combination with CSA, a single characteristic exposure value for each participant was difficult to derive. For each participant, a combined metric was calculated where the exposure following each combination of treatments was weighted by the number of days for each regimen. The overall median  $AUC_{ss}$  was predicted to be 49,200 ng·h/ml, with a 90% PI of 26,900–87,400 ng·h/ml.

In summary, letermovir steady-state PK in HSCT recipients was well-described by a two-compartment model with linear elimination and absorption. The model sufficiently described letermovir PK following oral or i.v. administration, alone or in combination with CSA. Data collected from healthy phase I study participants following single-dose and multiple-dose administrations of oral and i.v. letermovir were described by a four-compartment model with concentration-dependent nonlinear clearance and distribution, auto-induction of clearance, and a TCAM to describe absorption after oral administration. Intrinsic covariates were found not to affect letermovir PK to a clinically significant extent. These analyses indicate that letermovir PK are similar in HSCT recipients and healthy participants, differing only with respect to bioavailability and absorption rate. There was consistency between the two models in characterizing letermovir PK at clinical doses, further supporting the suitability of the HSCT recipient PK model for predicting exposure for exposure–response analysis to support dose selection.

## ACKNOWLEDGMENTS

The authors thank Randi Leavitt and Julie Stone, employees of Merck Sharp & Dohme Corp., a subsidiary of Merck & Co., Inc., Kenilworth, NJ, USA, for review and discussion, Bhavna Kantesaria, Ming Xu, Richard Moreton, and Linghui Zhang, employees of Merck Sharp & Dohme Corp., a subsidiary of Merck & Co., Inc., Kenilworth, NJ, USA, and Jan

Huissman, employee of qPharmetra, for their contributions to PK data generation and assembly. Medical writing support, under the direction of the authors, was provided by Paul O'Neill, PhD, of CMC AFFINITY, McCann Health Medical Communications, in accordance with Good Publication Practice (GPP3) guidelines. This assistance was funded by Merck Sharp & Dohme Corp., a subsidiary of Merck & Co., Inc., Kenilworth, NJ, USA.

### CONFLICT OF INTEREST

Marita Prohn is an employee of qPharmetra and a former employee of Merck Sharp & Dohme Corp., a subsidiary of Merck & Co., Inc., Kenilworth, NJ, USA. Anders Viberg and Kevin Dykstra are former employees of qPharmetra. Da Zhang, Casey Davis, Sreeraj Macha, Philip Sabato, Dinesh de Alwis, Marian Iwamoto, Craig Fancourt, and Carlyn R. Cho are current or former employees of Merck Sharp & Dohme Corp., a subsidiary of Merck & Co., Inc., Kenilworth, NJ, USA, and may own stock and/or stock options in Merck & Co., Inc., Kenilworth, NJ, USA.

### AUTHOR CONTRIBUTIONS

All authors wrote the manuscript. M.P., K.D., S.M., and C.R.C. designed the research. M.P., D.Z., and M.I. performed the research. M.P., A.V., D.Z., K.D., S.M., P.S., and C.R.C. analyzed the data.

### DATA AVAILABILITY STATEMENT

Merck Sharp & Dohme Corp., a subsidiary of Merck & Co., Inc., Kenilworth, NJ, USA (MSD) is committed to providing qualified scientific researchers access to anonymized patient-level data and clinical study reports from the company's clinical trials for the purpose of conducting legitimate scientific research. The company is also obligated to protect the rights and privacy of trial participants and, as such, has a procedure in place for evaluating and fulfilling requests for sharing company clinical trial data with qualified external scientific researchers. The process includes submission of data requests to the MSD data sharing website available at: [http://engagezone.msd.com/ds\\_documentation.php](http://engagezone.msd.com/ds_documentation.php). Data will be made available for request after product approval in the US and EU or after product development is discontinued. There are circumstances that may prevent MSD from sharing the requested data.

### FDA DISCLAIMER

The opinions expressed in this paper are those of the authors and should not be interpreted as the position of the US Food and Drug Administration.

### REFERENCES

1. Ljungman P, Hakki M, Boeckh M. Cytomegalovirus in hematopoietic stem cell transplant recipients. *Infect Dis Clin North Am*. 2010;24:319-337.
2. Jacobsen T, Sifontis N. Drug interactions and toxicities associated with the antiviral management of cytomegalovirus infection. *Am J Health Syst Pharm*. 2010;67:1417-1425.
3. Salzberger B, Bowden RA, Hackman RC, Davis C, Boeckh M. Neutropenia in allogeneic marrow transplant recipients receiving ganciclovir for prevention of cytomegalovirus disease: Risk factors and outcome. *Blood*. 1997;90:2502-2508.
4. Le Page AK, Jager MM, Iwasenko JM, Scott GM, Alain S, Rawlinson WD. Clinical aspects of cytomegalovirus antiviral resistance in solid organ transplant recipients. *Clin Infect Dis*. 2013;56:1018-1029.
5. Kotton CN, Kumar D, Caliendo AM, et al. The third international consensus guidelines on the management of cytomegalovirus in solid-organ transplantation. *Transplantation*. 2018;102:900-931.
6. Goldner T, Hewlett G, Ettischer N, Ruebsamen-Schaeff H, Zimmermann H, Lischka P. The novel anticytomegalovirus compound AIC246 (Letermovir) inhibits human cytomegalovirus replication through a specific antiviral mechanism that involves the viral terminase. *J Virol*. 2011;85:10884-10893.
7. Zimmermann H, Lischka P, Ruebsamen-Schaeff H. Letermovir (AIC246) a novel drug under development for prevention and treatment of cytomegalovirus infections acting via a novel mechanism of action. *Eur Infect Dis*. 2011;5:112-114.
8. Chemaly RF, Ullmann AJ, Stoelben S, et al. Letermovir for cytomegalovirus prophylaxis in hematopoietic-cell transplantation. *N Engl J Med*. 2014;370:1781-1789.
9. Merck & Co. Inc. Prevymis™ prescribing information. 2019. [https://www.merck.com/product/usa/pi\\_circulars/p/prevymis/prevymis\\_pi.pdf](https://www.merck.com/product/usa/pi_circulars/p/prevymis/prevymis_pi.pdf). Accessed February 12, 2020.
10. Merck Sharp & Dohme Ltd., London, UK. Prevymis summary of product characteristics. 2017. [http://www.ema.europa.eu/docs/en\\_GB/document\\_library/EPAR\\_-\\_Product\\_Information/human/004536/WC500241678.pdf](http://www.ema.europa.eu/docs/en_GB/document_library/EPAR_-_Product_Information/human/004536/WC500241678.pdf). Accessed February 12, 2020.
11. Marty FM, Ljungman P, Chemaly RF, et al. Letermovir prophylaxis for cytomegalovirus in hematopoietic-cell transplantation. *N Engl J Med*. 2017;377:2433-2444.
12. Kropf D, Scheuenpflug J, Erb-Zohar K, et al. Pharmacokinetics and safety of letermovir, a novel anti-human cytomegalovirus drug, in patients with renal impairment. *Br J Clin Pharmacol*. 2017;83:1944-1953.
13. Kropf D, von Richter O, Stobernack HP, Rübsamen-Schaeff H, Zimmermann H. Pharmacokinetics and safety of letermovir coadministered with cyclosporine A or tacrolimus in healthy subjects. *Clin Pharmacol Drug Dev*. 2018;7:9-21.
14. Stoelben S, Arns W, Renders L, et al. Preemptive treatment of cytomegalovirus infection in kidney transplant recipients with letermovir: Results of a phase 2a study. *Transpl Int*. 2014;27:77-86.
15. Erb-Zohar K, Kropf D, Scheuenpflug J, et al. Intravenous hydroxypropyl  $\beta$ -cyclodextrin formulation of letermovir: A phase I, randomized, single-ascending, and multiple-dose trial. *Clin Trans Sci*. 2017;10:487-495.
16. McCrea JB, Macha S, Adedoyin A, et al. Pharmacokinetic drug-drug interactions between letermovir and the immunosuppressants cyclosporine, tacrolimus, sirolimus, and mycophenolate mofetil. *J Clin Pharmacol*. 2019;59:1331-1339.
17. Bergstrand M, Hooker AC, Wallin JE, Karlsson MO. Prediction-corrected visual predictive checks for diagnosing nonlinear mixed-effects models. *AAPS J*. 2011;13:143-151.

18. Lindbom L, Pihlgren P, Jonsson EN. PsN-Toolkit—a collection of computer intensive statistical methods for non-linear mixed effect modeling using NONMEM. *Comput Methods Programs Biomed.* 2005;79:241-257.
19. Matis JH, Wehrly TE. Generalized stochastic compartmental models with Erlang transit times. *J Pharmacokinet Biopharm.* 1990;18:589-607.
20. Savic RM, Jonker DM, Kerbusch T, Karlsson MO. Implementation of a transit compartment model for describing drug absorption in pharmacokinetic studies. *J Pharmacokinet Pharmacodyn.* 2007;34:711-726.
21. Jacobson PA, Ng J, Green KG, Rogosheske J, Brundage R. Posttransplant day significantly influences pharmacokinetics of cyclosporine after hematopoietic stem cell transplantation. *Biol Blood Marrow Transplant.* 2003;9:304-311.
22. Zhang D, Chow DS. Clinical pharmacokinetics of mycophenolic acid in hematopoietic stem cell transplantation recipients. *Eur J Drug Metab Pharmacokinet.* 2017;42:183-189.
23. Vanstraelen K, Prattes J, Maertens J, et al. Posaconazole plasma exposure correlated to intestinal mucositis in allogeneic stem cell transplant patients. *Eur J Clin Pharmacol.* 2016;72:953-963.
24. Chen D, Hartmann G, Menzel K, Cho C. Development of a physiologically-based pharmacokinetic model to understand the nonlinear pharmacokinetics of letermovir and exposure differences between populations. *Drug Metab Pharmacokinet.* 2018;33:S36.
25. Fancourt C, Cho C, Viberg A, Prohn M, Dykstra K, Macha S. Comparison of two population pharmacokinetic models characterizing letermovir pharmacokinetics separately in healthy subjects and patients. *Abstracts for the Ninth American Conference on Pharmacometrics (ACoP9).* W-091 ed; 2018.

## SUPPORTING INFORMATION

Additional supporting information may be found online in the Supporting Information section.

**How to cite this article:** Prohn M, Viberg A, Zhang D, et al. Population pharmacokinetics of letermovir following oral and intravenous administration in healthy participants and allogeneic hematopoietic cell transplantation recipients. *CPT Pharmacometrics Syst. Pharmacol.* 2021;10:255–267. <https://doi.org/10.1002/psp4.12593>